

1 **A coastal vulnerability assessment for planning climate resilient infrastructure.**

2
3 Jennifer M. Brown^{1*}, Karyn Morrissey^{2,3}, Philip Knight², Thomas D. Prime^{1,2}, Luis Pedro Almeida^{4,5},
4 Gerd Masselink⁴, Cai O. Bird^{6,2}, Douglas Dodds⁷, Andrew J. Plater²

5
6 ¹The National Oceanography Centre, Marine Physics and Ocean Climate, Liverpool, UK

7 ²University of Liverpool, Department of Geography and Planning, Liverpool, UK

8 ³University of Exeter, Medical School, European Centre for Environment and Human Health, Truro
9 UK

10 ⁴Plymouth University, School of Biological & Marine Sciences Plymouth, UK

11 ⁵Centre National d'Études Spatiales (CNES-LEGOS), Toulouse, France

12 ⁶Marlan Maritime Technologies Ltd, Liverpool, UK

13 ⁷National Grid, Engineering & Asset Management, ETO, Warwick, UK

14 *Corresponding author's email jebro@noc.ac.uk

16 **Highlights**

- 17
- 18 • Changing threats to coastal populations and infrastructure are found.
 - 19 • Features that enable coastal resilience are identified.
 - 20 • An approach to develop a stakeholder-focussed decision-support tool is presented.
 - 21 • Physical process understanding and real options analysis are combined.

22 **Abstract**

23 There is a good understanding of past and present coastal processes as a result of coastal
24 monitoring programmes within the UK. However, one of the key challenges for coastal managers
25 in the face of climate change is future coastal change and vulnerability of infrastructure and
26 communities to flooding. Drawing on a vulnerability-led and decision-centric framework (VL-DC)
27 a Decision Support Tool (DST) is developed which, combines new observations and modelling to
28 explore the future vulnerability to sea-level rise and storms for nuclear energy sites in Britain. The
29 combination of these numerical projections within the DST and a Real Options Analysis (ROA)
30 delivers essential support for: (i) improved response to extreme events and (ii) a strategy that
31 builds climate change resilience.

32

33

34 **Key words:** Decision Support Tool (DST); Real Options Analysis (ROA); Flood hazard modelling;
35 Storm impact monitoring; Human intervention.

36

37 1. Introduction

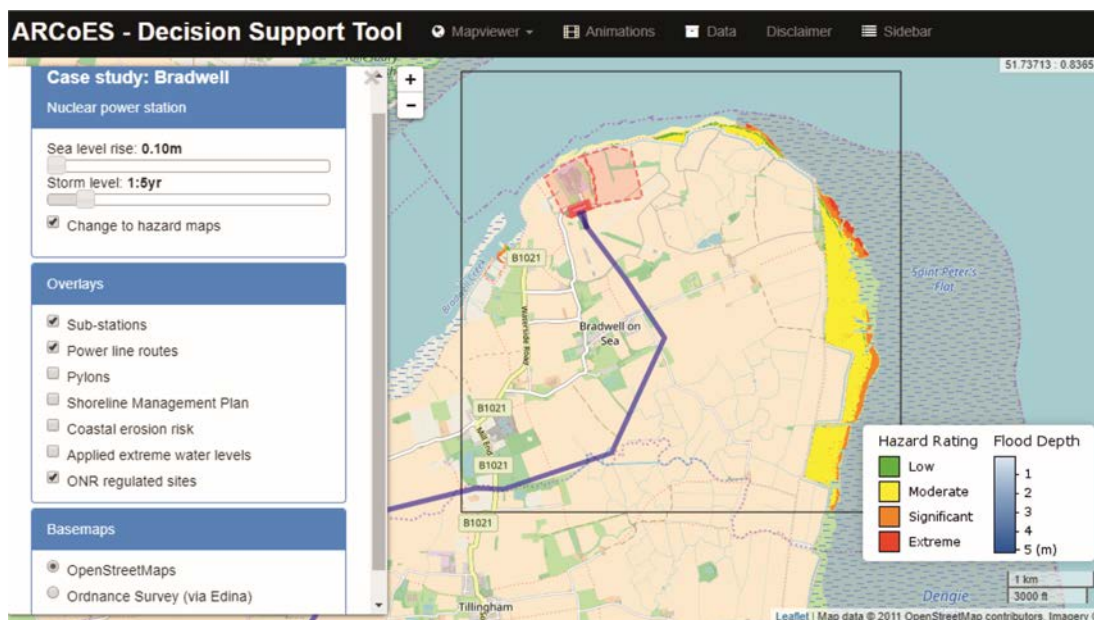
38 Energy security is a fundamental requirement for well-functioning modern societies (Morrissey et
39 al., 2018). Due to its prevalent location in coastal areas, climate change, sea-level rise and extreme
40 events represent significant challenges to the global energy infrastructure and supply chain
41 (Reichl et al., 2013; Morrissey et al., 2018; Prime et al., 2018). The UK Energy Networks
42 Association (ENA) identifies the biggest pressure to be from coastal flooding - if an electrical
43 substation is flooded costs in clean up and repair can be high, and on-going costs from disruption
44 and loss of supply have the potential to add to this significantly (Energy Network Association,
45 2009). There is already a good understanding of past and present coastal processes, particularly
46 at locations for present and planned nuclear power stations. However, to ensure that coastal
47 populations and the necessary infrastructure required to sustain these populations are resilient
48 in the future, tools that can inform adaptive management are required (Silva et al., 2017; Wadey
49 et al., 2017; Lam et al., 2017). However, this is a complex problem as shoreline resilience to
50 changes in the physical environment varies spatially and temporally in response to factors such as
51 changing beach volume (Castelle et al., 2015), reduction in sediment supply (Guangwei, 2011),
52 and the degradation of coastal wetlands (Lotzel et al., 2006), as well as to human interventions
53 that are socio-economically, politically and culturally determined (Ratter et al., 2016). To be
54 effective, management tools require the capacity to monitor and project a variety of interlinked
55 physical and societal processes including sea-level rise, storm magnitude/frequency relationships,
56 changing sediment budget (Brown et al., 2016) and population change and economic activity
57 (Prime et al., 2018).

58

59 Developed for the UK energy sector as part of the Adaptation and Resilience of Coastal Energy
60 Supply (ARCoES) project, this paper presents a web-based geospatial Decision-Support Tool (DST),
61 the ARCoES DST (Fig. 1). Leaflet, an open source Javascript library, is used to construct the DST to
62 enable the end user to interrogate the matrix of model results using slider bars and tick box
63 options to toggle between hazard or inundation maps and overlay different infrastructure or map
64 views (Knight et al., 2015). As described in this paper, the ARCoES DST is used in combination with

65 modelling and monitoring of different coastal environments to better understand future coastal
66 vulnerability. Drawing on the interdisciplinary skills of the ARCoES researchers, the ARCoES DST is
67 combined with an economic framework, Real Options Analysis (ROA), to provide an assessment
68 of when it is most cost-effective to implement a new management approach. From a policy
69 perspective, the data produced by the DST, when combined with a Real Options Framework can
70 be used to initiate discussions with coastal practitioners to identify how future vulnerability to
71 coastal flooding may be mitigated through appropriate and timely intervention and adaptation.
72 Importantly, although the methodology is designed for the nuclear energy sector the DST could
73 also be applied for other coastal management needs.

74



75

76 Fig. 1. The ARCoES DST, available at <http://arcoes-dst.liverpool.ac.uk/>.

77

78 Within this context, the aim of this paper is to demonstrate the usefulness of the ARCoES DST in
79 understanding the physical and economic impact of sea-level rise and storms across 4 nuclear
80 energy sites located along the coast of the UK. These sites include Seascale (representing Sellafield
81 in the northwest), Lilstock (representing Hinkley Point in the southwest), Sizewell (in the east),
82 and Bradwell (in the southeast). We also focus on Fleetwood (in the northwest) as an example of
83 its application to a coastal community. The paper continues as follows: the methods used to
84 deliver this holistic assessment are presented in Section 2. In Section 3 a selection of results to
85 demonstrate the application and capabilities of the resulting DST at different sites is provided. The
86 way in which this DST can be used to conceptualize shoreline management requirements to pose

87 questions at a high level for specialized studies to address is discussed in Section 4, before the
88 conclusions about the future resilience of UK coastal energy are drawn in Section 5.

89

90 **2. Site Descriptions**

91 Although applied to a number of locations, here we focus on five study sites with different coastal
92 geomorphology and hazard exposure. This national application demonstrates the development of
93 a DST for the management needs of an industry with infrastructure in multiple locations rather
94 than in response to site-specific coastal conditions. Each site requires a slightly different model
95 configuration (see Section 3) but uses the same approach.

96

97 The coastline at Seascale/Sellafield faces the Irish Sea, the actual location is quite exposed
98 (offshore $H_s, 10\% = 2$ m; max $H_s = 5.7$ m; data from British Oceanographic Data Centre (BODC) wave
99 buoy MCMBE-OFF 1974–1976), with a maximum tide range and 1% storm surge height during
100 winter of 7 m and 1 m, respectively. However, the beach morphology fronting the facility is
101 characterised by a reflective high tide gravel/cobble beach with an extremely dissipative sandy
102 intertidal zone. A storm monitored in January 2013 that more or less coincided with spring high
103 tide had therefore insignificant impact on the beach (Almeida et al., 2014).

104

105 At Lilstock/Hinkley Point, located in the Bristol Channel, the site is not fully exposed to the Atlantic
106 waves, but wave conditions can be relatively energetic (offshore $H_s, 10\% = 1.8$ m; max $H_s = 3.7$ m;
107 data from BODC wave buoy SEVERNEST A 1979–1981). This is a mega-tidal environment with a
108 maximum tide range of 10.7 m and a 1% storm surge height during winter of 0.8 m. However, in
109 common with Sellafield, the wide and low gradient intertidal zone, here a rocky platform instead
110 of a sandy beach, is extremely dissipative, limiting the wave energy levels impacting the high tide
111 gravel/cobble beach. A storm monitored in December 2013 had therefore very limited
112 morphological impact.

113

114 The gravel beach at Sizewell faces the North Sea. Wave conditions are relatively mild (offshore 10%
115 exceedance $H_s = 0.6$ m; max $H_s = 2.2$ m; data from BODC wave buoy ALDEBURG 1975–1977) and
116 the maximum tide range and 1% storm surge height during winter are 2.4 m and 1 m, respectively.
117 During the 5-year duration of the ARCoES project, not a single extreme wave event occurred at
118 Sizewell, but some measurements were made during a relatively modest storm event in March

119 2013. These revealed that the subtidal bar morphology at this site provides significant protection
120 to the high tide gravel beach from large waves and that the main morphological changes occurred
121 due to longshore sediment transport processes. The most significant wave events along the North
122 Sea coast are from the northeast quadrant, but Sizewell is partly sheltered from such storms
123 because the coastline aligns south-southwest to north-northeast, and potentially the most
124 damaging waves for Sizewell are extremely rare storm waves from the southeast. Interestingly,
125 the storm surge event in 2013, and which caused much erosion and flooding along the east coast
126 of England (Wadey et al., 2015), was not an event of significance at Sizewell where H_s at the peak
127 of the storm surge were < 1.5 m.

128

129 The Bradwell site is characterised by a narrow gravel coastal plain fronted by the silty tidal flat and
130 is located on the southern bank of the Blackwater estuary. The maximum tide range here is 4.8 m
131 and the 1% winter storm surge is 0.9 m. The site is extremely sheltered and this is demonstrated
132 by the results of a long-term deployment (Oct 2015 –Mar 2016) of pressure sensors at the base
133 of the gravel beach and around low tide level. Mean wave conditions were characterised by $H_s =$
134 0.1 m and the most energetic event that occurred during this period had a H_s of 0.45 m.

135

136 Observing the physical processes at the sites above has found that they have a low vulnerability
137 to storm impact. Seascale/Sellafield and Lilstock/Hinkley Point are relatively exposed sites, the key
138 aspect limiting their vulnerability to extreme wave events is their highly dissipative intertidal zone
139 (sand at Sellafield and rock at Hinkley Point). The very wide (> 200 m) and low-gradient (< 0.015)
140 surface fronting the high tide gravel/cobble beach and coastal structures at both sites greatly
141 reduces the wave energy levels and wave runup around high tide, and therefore the risk of
142 flooding and erosion, even under the largest offshore waves. Sizewell is sited such that it is not
143 exposed to the most frequent North Sea storm wave conditions from the northeast quadrant. In
144 addition, the low gradient and barred subtidal zone effectively dissipates storm wave energy, and
145 the high and wide inter- and supratidal gravel beach also provides a significant buffer to extreme
146 wave action. The site is perhaps most vulnerable to longer-term coastal dynamics, specifically
147 alongshore redistribution of sand and gravel due to littoral drift. Bradwell is sited in an extremely
148 sheltered location with very limited fetch and potential for wave generation. A low gradient
149 subtidal zone and gravel ridges also fronts the facility, which adds additional protection.

150

151 In addition to sites of nuclear infrastructure the ARCoES DST was also developed to assess
152 community vulnerability to coastal hazards. Our example site at Fleetwood, northwest England, is
153 used here to demonstrate how flood hazard management of a community's electricity distribution
154 has to consider the influence of shoreline management plans on the inland flood hazard to
155 electricity substations to ensure the supply is resilient. The coastal conditions at this site include
156 a mega-tidal regime (exceeding 10 m during spring tides), surge events that can reach 2 m and
157 offshore wave conditions that can exceed 5.5 m (Brown et al., 2010). Our study region has a 'hold
158 the line' shoreline management policy to protect the community from flood hazards. Within our
159 study area this policy is implemented by a sea wall, thus understanding when a future 'tipping
160 point' in wave overtopping hazard may occur for the existing scheme under rising sea levels is
161 important.

162

163 **3. ARCoES DST**

164 There is often a good understanding of past and present coastal processes as a result of coastal
165 monitoring programmes within the UK. However, one of the key challenges for managers in the
166 face of climate change, is future coastal change and vulnerability of infrastructure and
167 communities to flooding. A vulnerability-led and decision-centric framework (VL-DC) (Armstrong
168 et al., 2015), the ARCoES approach combines new observations and modelling to explore the
169 future vulnerability to sea-level rise and storms for nuclear energy sites in Britain. As will be
170 outlined below, the resulting DST provides inundation mapping via LISFLOOD-FP, XBeach, XBeach-
171 G and SWAB modelling. The data are then combined in a ROA framework to provide an
172 assessment of when it is most cost-effective to implement a new management approach.

173

174 *3.1 Inundation Mapping*

175 Inundation mapping is a key component of the ARCoES DST. While a general overview of the
176 model application is provided here, more detailed studies focusing on individual sites (e.g., Prime
177 et al., 2015a; 2015b; 2016) have considered sensitivity analysis of the model results to ensure the
178 approach is robust for the purpose of the DST. A "soft" coupling approach is adopted where a
179 storm impact model provides the input to an inundation model. Here we use models that are
180 frequently used in flood and erosion risk studies (e.g., Lewis et al., 2013; Phillips et al., 2017; Poate
181 et al., 2016).

182

183 LISFLOOD-FP (Bates et al., 2005) has been applied as a coastal inundation model to map depth,
184 extent and velocity of floodwaters for extreme coastal and riverine events under rising sea levels.
185 The horizontal model resolution varies from 20 m to 50 m depending on the size of the domain
186 (which range from sites of critical infrastructure to the regional scale for supply network
187 assessments) to allow efficient computation time and to capture the required level of detail for
188 the management needs. Data on the time-varying storm tide alone, or combined storm tide and
189 wave overwashing or overtopping volumes are used to generate the hazard imposed at the coastal
190 boundary within LISFLOOD-FP, which propagates the floodwater landward across the floodplain.
191 The positioning of the coastal boundary is domain dependent as is the boundary input data. At
192 sites where wave hazard is considered negligible the low water contour is imposed as the coastal
193 boundary and forced by storm tide water levels at 15 minute time intervals. At sites where wave
194 hazard is considered important, through overtopping or overwash, the crest of a defence line
195 (natural or engineered) is set as the coastal boundary and a wave resolving storm impact model
196 is used to provide the (10 minute average) inflow discharge. In all cases the implemented models
197 are run for a tidal cycle starting from low water. The inland model boundary is set some distance
198 from the coast to ensure the flood pathways and area of inundation are generally contained within
199 the domain. The boundary is set to allow through flow so under very extreme events the water is
200 not restricted in a way that will cause it to inaccurately build-up. For the Fleetwood case high river
201 flows have also been imposed as a discharge at the boundary points that cross the river Wyre (see
202 Prime et al., 2015a). This allows the user to explore a range of flood hazard combinations (sea-
203 level rise, coastal storms and high river flow).

204

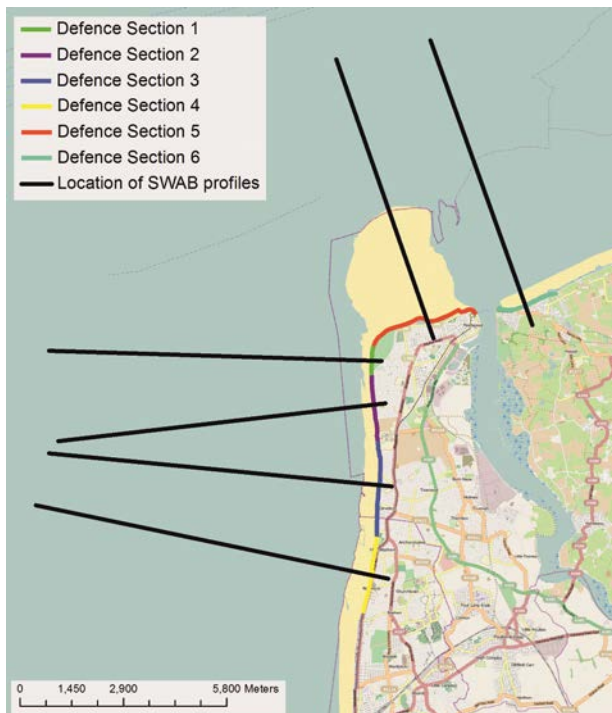
205 At sites with wave hazard, overwashing or overtopping volumes have been calculated for various
206 defences: hard engineered (SWAB, McCabe et al., 2013), sand dune (XBeach, Roelvink et al., 2010)
207 or gravel barrier (XBeach-G, McCall et al., 2014, 2015). The use of the XBeach and XBeach-G
208 models enables the role of storm-driven morphology and features within the cross-shore profile
209 to be considered within the impact assessment. These models are applied as 1DH (horizontal)
210 cross-shore profile models for present-day morphologies within the DST, while hypothetical future
211 morphologies (such as changes in saltmarsh extent, barrier beach morphologies or subtidal bar
212 geometries) are considered in more focused site-specific applications to determine potential
213 changes in a system's response to storm impact (e.g., Prime et al., 2015b). The Shallow Water
214 Boussinesq Model (SWAB) has also been used for a site with a sea wall (Prime et al., 2015a).

215 Although XBeach and XBeach-G can consider a fixed structure within the profile SWAB has been
216 developed and validated with field observations to account for random wave breaking, impact
217 and overtopping of sea walls (McCabe et al., 2013).

218

219 The initial profiles in the 1DH simulations are based on a combination of the latest available
220 bathymetric data and beach profile surveys obtained for the site. The modelled cross-shore
221 profiles have been selected to capture alongshore variability in the present-day coastal defence.
222 At sites of energy infrastructure with a natural defence (gravel barrier or dunes) a 1 km spacing
223 between the profiles with 50 m spacing closer to the nuclear power station is used to capture the
224 alongshore variability in the beach-barrier system (Prime et al., 2016). For sites with sea walls a
225 centrally positioned transect perpendicular to each defence section is chosen to simulate the
226 flood hazard for each of the different defence designs (Prime et al., 2015a). An example set-up is
227 shown in Fig. 2, where the sea wall provides protection to the local community behind. For sites
228 where the 1DH models have been used to incorporate wave impact the wave direction is always
229 assumed to be directly onshore to generate the worst case scenario.

230



231

232 Fig. 2. The LISFLOOD-FP model domain used to simulate flood hazard around the Fylde peninsula,
233 northwest England. SWAB is applied in this example for each cross-section to simulate the wave-
234 water inflow at the defence crest level (Prime et al., 2015a).

235

236 Within the ARCoES DST the flood maps were developed using data available to coastal managers.
237 This includes the most recently available airborne laser altimetry (LiDAR) collected by the
238 Environment Agency (EA) and observational data collected by national monitoring programs
239 where available. These data include shoreline profile information collected by the EA or local
240 authorities, the UK tide gauge network record (established in 1953), owned and operated by the
241 EA, and the WaveNet record, a UK network of wave buoys (established in 2002) operated by the
242 Centre for Environment Fisheries and Aquaculture Science (CEFAS). These real-time systems
243 provide a long-term data archive to which a joint probability analysis can be applied to generate
244 wave-water level combinations representative of a range of storm severities. Where observations
245 are not available tidal predictions are obtained from the POLTIPS3 software, available from the
246 national tide sea level facility, and wave data are obtained from long-term (40-year) hindcasts,
247 such as the UK Climate Predictions 09 (UKCP09, Lowe et al., 2009) and the global wave hindcast
248 produced in preparation of the European Centre for Medium Range Weather Forecasts (ECMWF,
249 2016) next reanalysis (ERA5).

250

251 Where observations are limited to within the last decade (e.g., wave monitoring) or where only
252 waves or water levels are monitored, archived data from climate modelling systems can be utilized
253 to lengthen the datasets. The longer the data record the greater the confidence in the extreme
254 value analysis. This research has used the European Centre for Medium-Range Weather Forecasts
255 (ECMWF) 30-year wave ECWAM cycle 41R1 model data to lengthen the wave records. These
256 numerical data are validated against existing wave observations prior to use in the analysis.

257

258 For the UK energy sector, events ranging from typical (1 in 1 year return period) to extreme (1 in
259 10,000 year return period) conditions are considered. The joint probability analysis is performed
260 using JOIN-SEA (Hawkes and Gouldby, 1998). This software uses the generalised Pareto
261 distribution (GPD) model and simultaneous records of significant wave height (H_s) and water level
262 (WL) at the time of the observed high water. In most cases the combined observational record
263 covered a period of the order of a decade, the limitation often being related to the deployment
264 of the wave buoy. For each return level a range of wave-water level conditions are generated.
265 These cover conditions that transition from lower WL and higher H_s to higher WL and lower H_s .
266 The conditions that pose greatest flood hazard along the probability curves are selected from an

267 ensemble of 1DH storm impact simulations that generate a range of inflow conditions to impose
268 into LISFLOOD-FP (Prime et al., 2016). This generates the database of flood maps behind the DST.
269 In this respect, the DST operates as a look-up table.

270

271 Once the required wave-water level combination has been ascertained a storm tide is created to
272 force the offshore model boundary. The storm tide comprises a spring tide and a surge curve,
273 available for all UK Class A tide gauge locations from the EA (McMillan et al., 2011). The surge
274 curve is used to scale the tide such that the total high WL reaches the required extreme value.
275 The time-varying water levels are combined with the required wave conditions within the 1DH
276 storm impact model. Although the H_s is kept constant, a JONSWAP (Joint North Sea Wave
277 Observation Project) spectrum is applied to create a time-varying wave field. This approach
278 represents the worst-case scenario as the wave conditions maintain the desired extreme value for
279 the duration of the simulation, a complete tidal cycle. An appropriate peak wave period (T_p) is
280 selected from the wave data for each H_s . At many sites around the UK there is a bimodal wave
281 climate related to the wind sea and swell wave components. For each wave condition the longest
282 T_p associated with each H_s is used to simulate the highest wave runup levels.

283

284 Future sea-level projections are incorporated into the still water level of each event to take into
285 consideration sea-level rise and explore future change in the inundation hazard. The projections
286 are chosen to represent the high-end emission scenarios up to 2500AD (Jevrejeva et al., 2012).
287 Incremental increases in mean sea level are considered at 10 cm intervals up to a rise of 2 m and
288 then at 25 cm intervals to a rise of 5.5 m (Knight et al., 2015). The higher resolution is considered
289 for levels representing plausible projections that could occur over the next 100 years, consistent
290 with the long-term shoreline management planning framework. A lower resolution is then applied
291 for the more bespoke longer term (c. 500 year) projections for the energy industry.

292

293

294 *3.2 Monitoring*

295 Alongside the numerical applications, storm surveys were performed at three nuclear sites across
296 the UK, including Seascale (representing Sellafield in the northwest), Lilstock (representing
297 Hinkley Point in the southwest) and Sizewell (in the east), as well as a long-term wave gauge
298 deployment at Bradwell (in the southeast). This extreme event monitoring is used to assess the

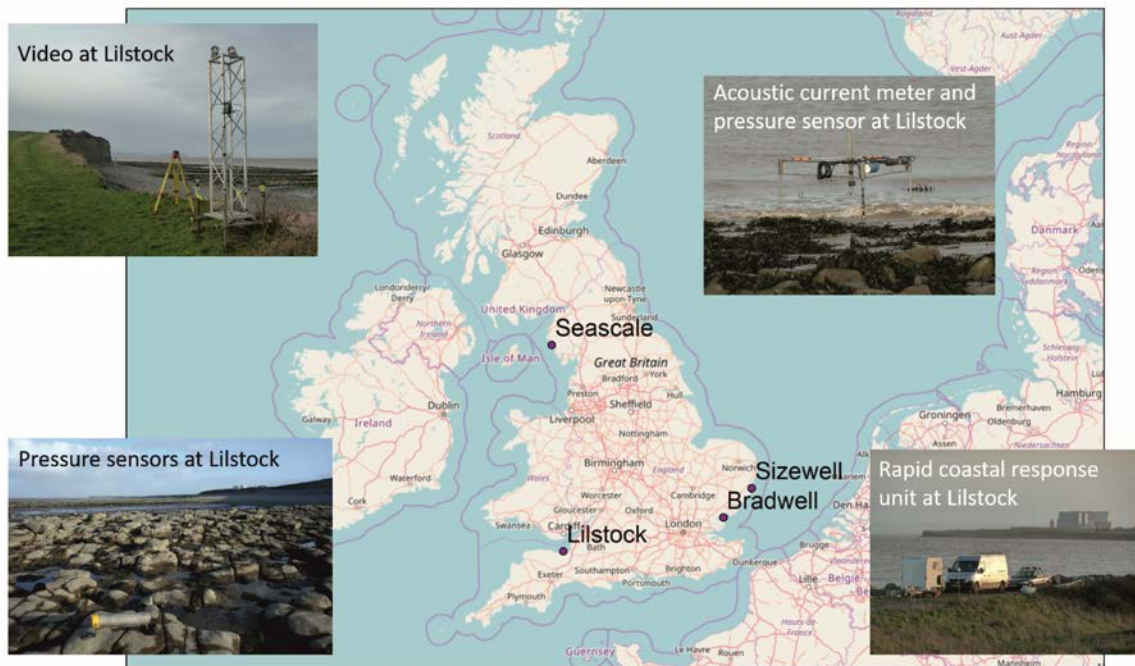
299 present-day vulnerability and disturbance-recovery behaviours of the sites. In order to
300 compliment short-term survey campaigns that aim to characterise coastal response to storms, a
301 cost-effective method of providing continuous observation of morphological change by
302 automatically mapping large coastal areas has also been developed using a standard marine
303 navigational radar (Bell et al., 2016; Bird et al., 2017a).

304

305 *3.2.1 Surveys*

306 Storm surveys over a tidal cycle were used to assess the response of different coastal systems and
307 identify features that make them resilient or resistant to storm impact. During an event pre-,
308 during and post-storm topographic data were collected (using a dGPS on a staff pole at low tide)
309 alongside in-situ measurements and remote sensing observations. The in-situ instruments (e.g.,
310 Fig. 3) were deployed pre-storm and retrieved after the storm. These included two low water
311 scaffold rigs with pressure transducers and current meters together with five scaffold tubes with
312 pressure transducers deployed alongshore at equal spacing (< 1 km) on the intertidal terrace.
313 These instruments recorded the wave and tide elevations and the current velocities during the
314 storm. Remote sensing techniques included a tower with two video cameras and a second tower
315 with a laser-scanner. The video cameras were positioned to continuously record alongshore
316 variability of wave runup during the storm (Poate et al., 2016). The laser-scanner tower was
317 deployed on the beach face to measure morphological change and swash hydrodynamics along a
318 cross-shore transect throughout the storm (Almeida et al., 2015; Almeida et al., 2017).

319



320

321 Fig. 3. Location map of the storm survey sites and examples of the instrumented rigs and towers
 322 deployed.

323

324 *3.2.2 Long-term monitoring*

325 A new monitoring technique has been deployed, which uses a radar-imaged sea surface and an
 326 accurate record of tidal elevations (such as a nearby tide gauge) as an altimeter to measure tidally-
 327 driven water level elevations at each pixel in a radar scan. By knowing the position of the waterline
 328 and the tidal elevation a bathymetric survey of the intertidal area can be produced. This
 329 methodology was used to observe seasonal changes in morphology over a 3-year period and
 330 assess storm impacts on beach volume and intertidal bedforms (Bird et al., 2017a). With the
 331 ambition of applying this radar technique to multiple locations a semi-mobile radar survey system
 332 has been developed during the ARCoES project by *Marlan Maritime Technologies Ltd*. This system
 333 is powered by solar panels and a wind turbine and provides a stable radar tower, CCTV camera
 334 and data recorder, enabling coastlines with limited power infrastructure to be monitored
 335 effectively. This system continuously monitors beach topography within a few kilometres of the
 336 radar for the entire duration of the deployment, which can then potentially update intertidal
 337 bathymetry and waterline levels in near real-time. Study sites are shown in Fig. 4.

338



339

340 Fig. 4. Location map of the radar monitoring sites and the radar systems deployed.

341

342 A previous application to the Dee estuary, northwest England, has demonstrated the capability of
343 the radar to monitor complex geomorphological environments (Bird et al., 2017b). The tidal range
344 in this estuary is in excess of 10 m on high spring tides. The morphology is very complex and
345 includes large areas of intertidal sandflats, subtidal channels, mud banks, saltmarshes and rock
346 outcrops. Using a 2.5 m radar antenna intertidal topography was derived with a 3 m spatial
347 resolution over a 4 km range from the radar. Comparison with LiDAR showed radar-based system
348 was able to derive the major features of the topography including complex channels and bedforms
349 with a vertical accuracy of +/- 20 cm (although limitations with the LiDAR data should also be
350 acknowledged in any error analysis) (Bell et al., 2016). This surveying system therefore provides
351 advanced warning of adverse morphological change, volumetric information on sediment
352 movements (especially useful for monitoring beach nourishment schemes or identifying erosion
353 hotspots), bedform migration and broad-scale indications of a beach system health. Following the
354 development of this rapidly deployable remote-sensing survey platform (Rapidar), planned winter
355 deployments at sites of critical energy infrastructure (2017-18 for Minsmere, E coast UK, and
356 2018-19 for Dungeness, SE coast UK) will collect data to assess longer-term resilience of these
357 sites. These will also be complemented by additional storm surveys to assess the response of

358 these coastal systems to a winter season. This will help to identify and assess the role of shoreline
359 response and morphological evolution within flood hazard assessments, enabling better
360 understanding of some of the uncertainty surrounding modelled flood maps.

361

362 *3.2.3 Real Options Approach (ROA)*

363 The financial viability of investment projects or the selection of investment alternatives is typically
364 assessed by cost–benefit analysis. The most widely used method is updating the future cash flows
365 generated by the coastal scheme. This method is often referred as Discounted Cash Flow (DCF).
366 However, it is widely acknowledged that the DCF leads to suboptimal decisions when irreversible
367 investments are subjected to uncertainty (Pringles et al., 2015), such as large-scale infrastructure
368 investment. Parallel to the modelling and monitoring of the physical processes, a Real Options
369 Analysis (ROA) was developed to identify which energy infrastructure will benefit from flood
370 management investment, and the optimal time to invest in this infrastructure (Prime et al., 2018).
371 ROA is an adaptation of financial options analysis applied to valuing of physical or real assets
372 (Pringles et al., 2015). ROA assesses the implied value of flexibility that is embedded in many
373 investment projects. Flexibility acknowledges that investment plans are modified or deferred in
374 response to the arrival of new (though never complete) information or until the uncertainty is
375 fully resolved (Pringles et al., 2015). Using Monte Carlo simulation, the ROA values the options to
376 defer or invest based on a set of pre-defined decision rules and option valuation (see for example
377 Pringles et al., 2015). The analysis provided by the ROA is used to form a cost-benefit decision-
378 support tree.

379

380 The next section presents a series of applications of the ARCoES DST to demonstrate the versatility
381 of information that can be generated for planning coastal adaptation to climate change.

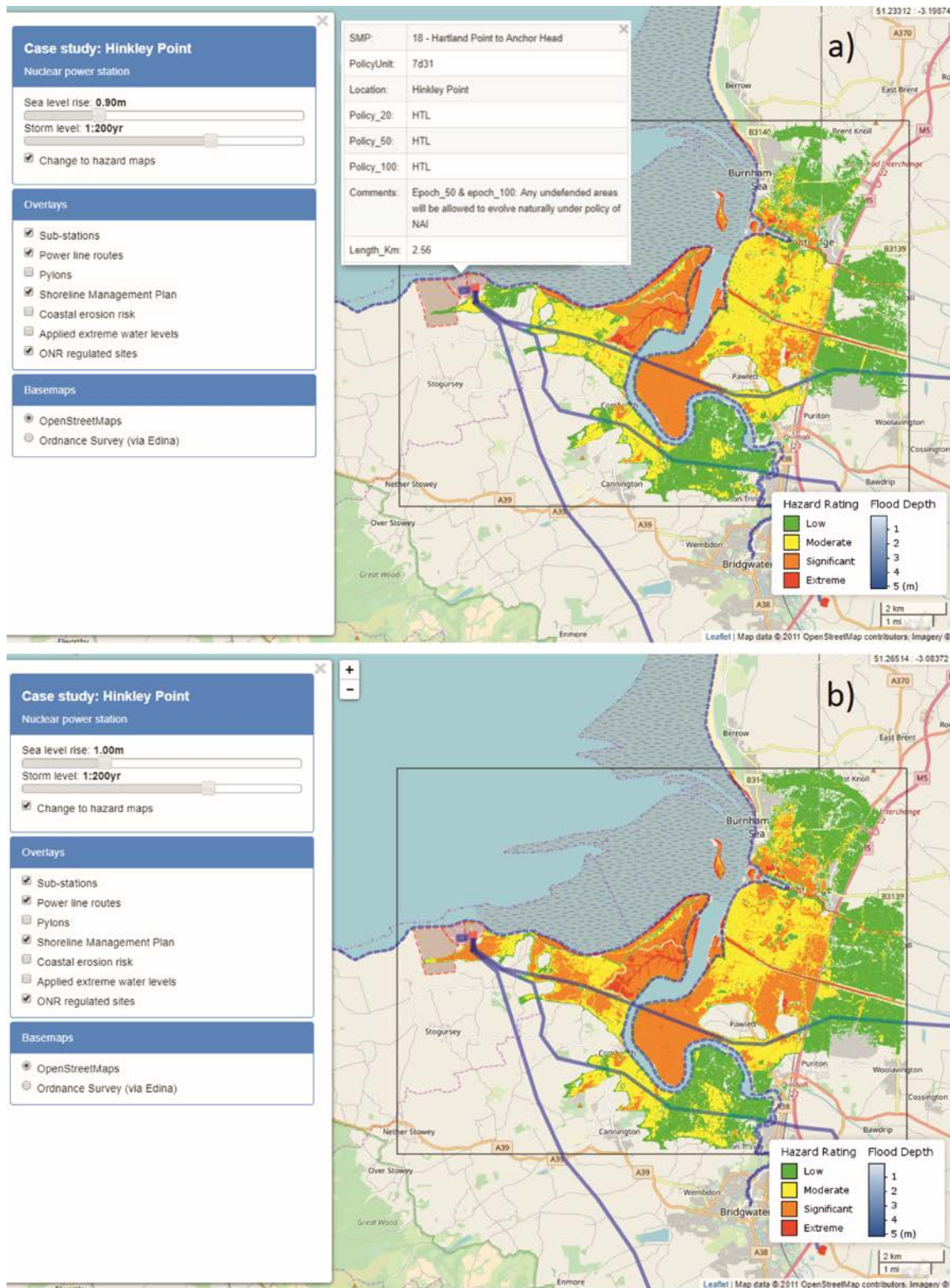
382

383 **3. Results**

384 *3.1 ARCoES DST*

385 The examples presented use LISFLOOD-FP (alone) in applications within the Bristol Channel and
386 Severn Estuary, southwest England. At Hinkley Point (Fig. 5) the shoreline management policy is
387 ‘hold the line’ (HTL Fig. 5a). By selecting a 1 in 200 year storm condition, typical of UK defence
388 standards, we identify a tipping point in the storm hazard rating to people (from low/moderate,
389 Fig. 5a, to significant, Fig. 5b, for road and power line route access) at around 1 m of sea–level

390 rise. At this site the flood hazard occurs due to inundation of lowlands towards the east of the site.
391 This type of information highlights the need to reassess operational strategies in the future,
392 particularly for first responders or workers using access routes or working on the electricity
393 transmission lines.



394

395

396

397

Fig. 5. Hinkley Point, showing a tipping point in the hazard to people from moderate to significant over access and electricity routes for a 1 in 200 year storm event and a change in mean sea level from a) 0.9 m to b) 1.0 m. Panel a also shows a pop-up window displaying the SMP metadata for

398 a defence section fronting the nuclear power station.

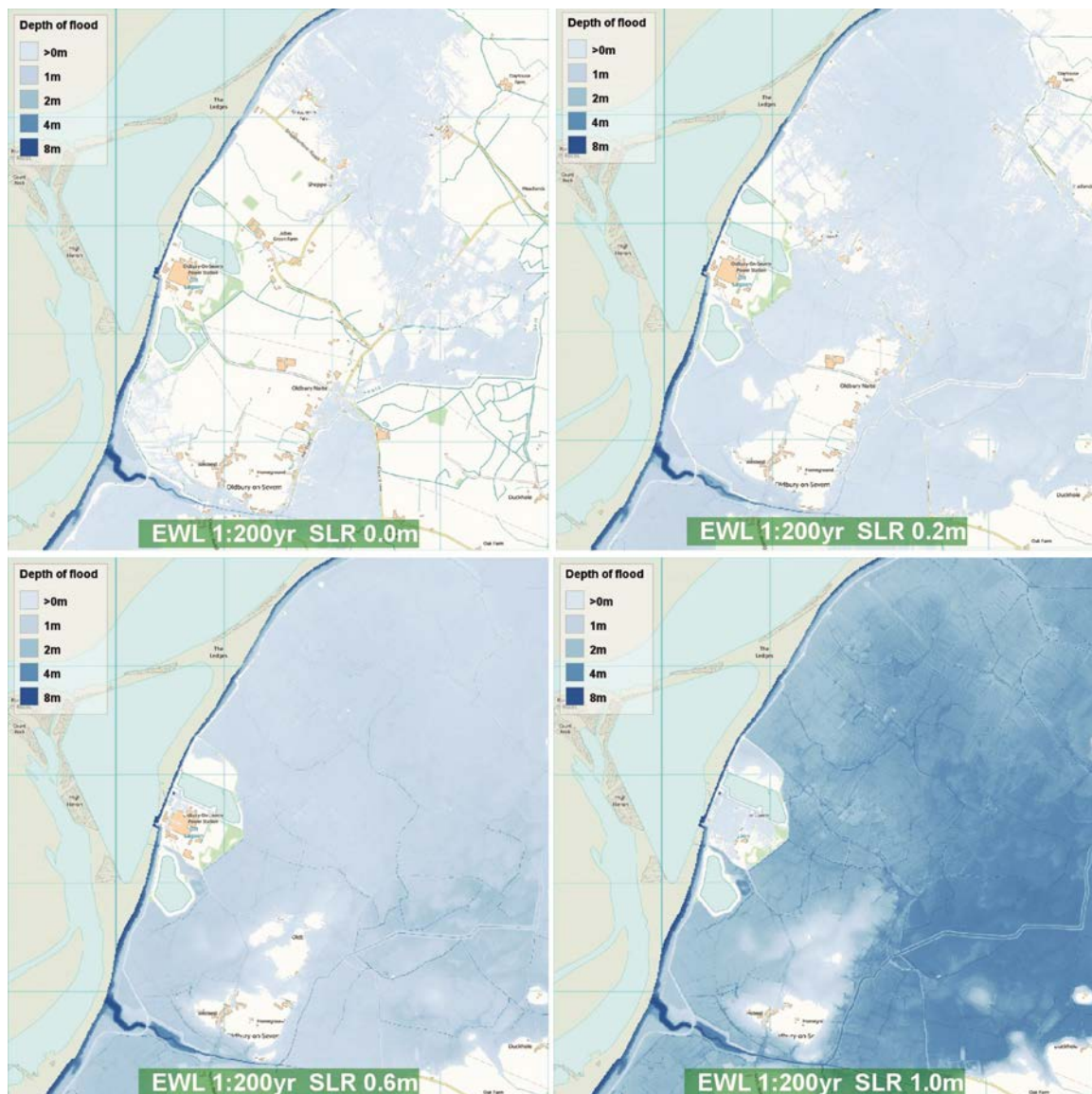
399

400 Animations are also available online for incremental sea-level rise and storm return period for
401 certain nuclear power station sites. Fig. 6 shows screen shots of the online animations for the
402 Magnox nuclear power station at Oldbury-on-Severn. The screen shots show increasing sea-level
403 rise and a constant 1:200 year storm level. The base map used for these images in Ordnance
404 Survey (OS, 2014). A 1:200 year storm level under present-day sea level (no increase) results in
405 inundation of agricultural land of less than 1 m. A 1:200 year event, accompanied by 0.2 m sea-
406 level rise results in more extensive inundation. However, the depth of inundation remains up to 1
407 m. The Oldbury-on-Severn site remains unaffected, as do some residential properties in the towns
408 of Oldbury-on-Severn and Oldbury Naite to the south. Around 0.6 m sea-level rise results in a
409 greater extent of inundation up to 1 m, particularly agricultural land to the southeast of the model
410 domain. Again, the nuclear site remains unaffected as well as some small areas around Oldbury-
411 on-Severn. Widespread inundation results from 1.0 m sea-level rise and low lying inland areas
412 become vulnerable as the flood water propagation is no longer restricted to limited pathways
413 during tidal high water. All transport and access routes within the area are flooded, as well as local
414 amenities, agricultural land and residential properties. These images show how the DST can be
415 used to simulate increasing sea-level rise superimposed on a 1:200 year event and the resulting
416 depth and extent of inundation, and thus identify where the vulnerability to flooding undergoes
417 a step change. This information is simulated with no change to present-day flood defence. It can
418 therefore identify where intervention may be required in the future, showing flood pathways to
419 help inform the optimal locations to invest in defence infrastructure.

420

421

422



423

424 Fig. 6. Animation screen shot of a scenario with a 1:200 year extreme water level (EWL) and 0.0
 425 m, 0.2 m, 0.6 m and 1.0 m sea-level rise (SLR) for the Oldbury model domain.

426

427 The DST is currently set-up to provide a simplified estimate of costs calculated from a depth-
 428 damage curve for different land uses considering inundation by saltwater (Fig. 7a). The DST
 429 displays the flooded area (km²) and cost (£M) for arable land, residential housing, roads, industry
 430 and the total area of inundation for the selected storm event and sea-level value. Using this
 431 information appropriate timeframes to implement new management strategies based on the
 432 relative costs of flooding and the benefits of implementing resilience measures can be planned
 433 (Prime et al., 2015a).

434

435 *3.2 Real Options Analysis (ROA)*

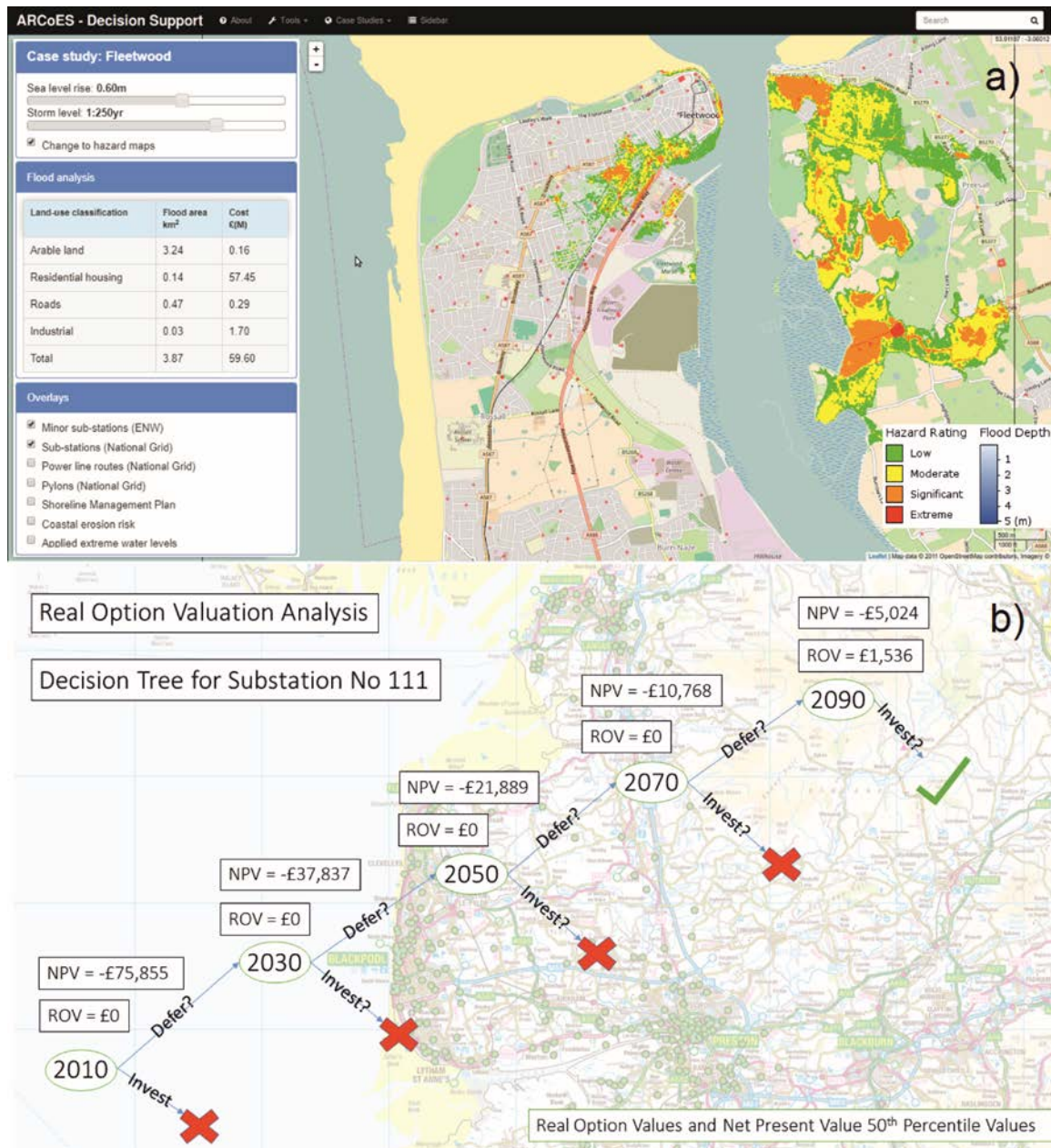
436 By identifying electricity distribution substations that are vulnerable to future flooding using the
437 DST a ROA can be applied to assess when the implementation of any resilience measures would
438 be cost-effective. The ROA combines the flood hazard exposure maps simulated for the sea-level
439 projections with the economic data associated with the investment decision such as inflation,
440 building costs, maintenance costs, clean-up costs and savings in relation to deferring a project
441 (Prime et al., 2018). Fig. 7b illustrates a classic Net Present Value (NPV) calculation based on the
442 most widely used investment decision tool, Discounted Cash Flow (DCF) analysis. According to
443 DCF-based calculation any substation that has a positive value should go ahead with flood defence
444 investment. However, NPV calculations based on DCF approaches do not value any flexibility in
445 the management process. Using ROA a flexible NPV is also calculated. Based on the more flexible
446 ROA methods, investment in flood defense for substation 111 should only go ahead in 2090.

447

448

449

450



451

452 Fig. 7. Examples of a) the DST cost-benefit information for Fleetwood, northwest England, (the red
453 symbols indicating where sub-stations are present) and b) the real options analysis decision tree
454 for a substation in the northwest England.

455

456 3.3 Monitoring

457 While the DST explores future scenarios identifying when tipping points in flood hazard for the
458 current management practice occur and the ROA enables assessment of when it is most cost-
459 effective to implement a new management approach, observations inform us of the present-day
460 disturbance-recovery behaviours of coastal environments (cf. Almeida et al., 2015). The ARCoES

461 project found that all four nuclear power station sites that were observed (see Section 2) currently
462 experience limited vulnerability to extreme storm events due to the combination of their siting
463 and geomorphology, as well as any site-specific interventions required as part of their pre-
464 operational and operational safety cases as a requirement of their licencing approval.

465

466 From this understanding we can cast the coastal flooding and erosion risk to nuclear power station
467 into a Source – Pathway – Receptor framework (Narayan et al., 2012; Sayers et al., 2002) and make
468 two general statements. Firstly, all nuclear power station locations have limited potential for the
469 occurrence of extreme wave conditions (i.e., Source) due to their siting. At the same time, the
470 sites have a common morphology (i.e., Pathway), characterised by a reflective and permeable
471 gravel/cobble high tide beach fronted by a wide and low gradient dissipative feature. This ensures
472 that even if the site experiences extreme wave energy levels, potential damage to the nuclear
473 power station site (i.e., Receptor) due to flooding and erosion would be limited. With uncertainty
474 surrounding the consequence of climate change and sea-level rise (the Source) at the coast,
475 monitoring of the morphology (Pathway) is recommended, using techniques such as Rapidar, to
476 provide early warning to trigger a review of the current management strategy to maintain the
477 required standard of protection (to the Receptor). Through understanding of the present-day
478 processes, critical evolution within the system can be identified for consideration in sensitivity
479 modelling using the models that make up the DST. One example would be the update and
480 exploration of time-evolving beach profiles within the numerical approach that generates the
481 hazard maps. Such studies continued study will highlight areas for continued development within
482 the DST.

483

484 **4. Conclusions**

485 The ARCoES DST and parallel ROA presented in this paper provide a resource that can be used to
486 initiate discussions with coastal practitioners to identify how future vulnerability to coastal
487 flooding may be mitigated through appropriate and timely intervention and adaptation. Such a
488 forum for dialogue is required to improve the transfer of knowledge between costal researchers
489 and decision-makers, to enable science based evidence to underpin choices made when setting
490 new coastal management strategies. The DST enables maps of potential flooding, and associated
491 costs, from increments of sea-level rise and storm magnitude to be explored by a wide range of
492 users to identify key locations and ‘tipping points’ where and when the increased vulnerability to

493 flooding challenges current operations, emergency plans and long-term management strategy.
494 When combined with understanding gained from present day observations informed monitoring
495 programmes to support management decisions can be put in place and site inspections can be
496 focused on assessing geomorphic change that has the potential to change a sites vulnerability to
497 storm impact. The detailed understanding of the local processes also allows the limitations of the
498 'static' morphology within the DST to be put in context though the identification of how
499 uncertainty within the mapped results could occur. A key area for expansion of the ARCoES
500 framework would be to incorporate shoreline evolution within the projections of future coastal
501 flood hazard. By using freely accessible models and mapping systems within the DST continued
502 development can be facilitated, enabling incorporation of such information in the future.

503

504 Within a policy context, project outputs have already provided practice and policy
505 recommendations for national and regional decision-makers on building coastal resilience to sea-
506 level rise and storms (please see the Living With Environmental Change (LWEC) partnership policy
507 and practice notes, Plater and Brown, 2016). In this respect, the DST and associated resources
508 provide a framework for engagement and dialogue across research and stakeholder communities
509 for the co-production of future plans (e.g., Armstrong et al., 2015). Over the longer term, the DST
510 provides energy infrastructure stakeholders with a roadmap for planned investments that address
511 resilience to future change in sea level and extreme events. This would include measures such as
512 the relocation of substations, raising transformers and other hardware above ground, and
513 replacing ageing assets (e.g. circuit breakers) that may be more sensitive to water. The DST
514 therefore delivers essential support for: (i) improved response to extreme events and (ii) a strategy
515 that builds climate change resilience. Both offer the consumer greater confidence in the constancy
516 of energy supply and an awareness that their money is being spent effectively in combating
517 present and future risks from flooding.

518

519 Finally, the ARCoES DST platform is an effective example of inter-disciplinary collaboration across
520 physical, natural, and social sciences on one axis, and across research, energy and infrastructure
521 sectors, coastal management authorities, environmental regulators, and coastal communities on
522 another. Interactive dissemination of the DST has revealed its value in discussions that centre on:
523 (i) future changes in coastal geomorphology and how this may be managed to promote 'natural'
524 coastal resilience, (ii) engagement of stakeholders with projections of flooding due to sea-level

525 rise and other forcing factors, and uncertainties therein; and (iii) interventions that mitigate
526 impacts in an appropriate (according to location and scale of challenge), timely and cost-effective
527 way. The DST is therefore presented as a resource for framing dialogue and exploring solutions,
528 rather than providing simplistic answers out of context. Rather than this being viewed in negative
529 terms by decision makers, the DST has been received positively as providing a focus for the sharing
530 of knowledge, perspectives and priorities.

531

532 **Acknowledgements**

533 This research was funded through the EPSRC-funded ARCC ARCoES project (EPSRC EP/I035390/1),
534 NERC-funded project “Sandscaping for Mitigating Coastal Flood and Erosion Risk to Energy
535 Infrastructure on Gravel Shorelines: a case study approach” (NE/M008061/1), and the EPSRC IAA
536 (Impact Acceleration Account) scheme, which funded the project ‘Use of Sandscaping
537 Interventions for Coastal Protection’. It builds on conference presentations given at Coastal
538 Dynamics 2017 in Denmark by Brown et al. (2017) and Lyddon et al. (2017). National Grid are also
539 thanked for their support and input to the development of the DST and for sharing knowledge in
540 relation to climate change and adaptation. Multiple projects associated to ARCoES have also
541 contributed to the new understanding and information behind the DST. The key PhD studentships
542 include: “The feasibility of mega-recharge projects for coastal resilience: physical, economic and
543 societal considerations” and “Physical, operational and economic resilience of coastal energy
544 networks.” We would like to thank Jean-Raymond Bidlot from the ECMWF for the provision of the
545 30-year wave ECWAM cycle 41R1 model hindcast dataset. In addition, we thank CEFAS for
546 providing the full datasets from WaveNet, and the National Tidal and Sea Level Facility for
547 providing the tide gauge data archived with the BODC.

548

549 **References**

- 550 Almeida, L.P., Masselink, G., McCall, R., Russell, P., 2017. Storm overwash of a gravel barrier: field
551 measurements and XBeach-G modelling. *Coastal Engineering*, 120, 22–35.
- 552 Almeida, L.P., Masselink, G., Russell, P., Davidson, M., McCall, R., Poate, T., 2014. Swash zone
553 morphodynamics of coarse-grained beaches during energetic wave conditions. In:
554 Proceedings of the International Conference on Coastal Engineering, Seoul, South Korea,
555 2014.
- 556 Almeida, L.P., Masselink, G., Russell, P., Davidson, M., 2015. Observations of gravel beach

557 dynamics during high energy wave conditions using a laser scanner. *Geomorphology*, 228,
558 15–27.

559 Armstrong, J., Wilby, R., Nicholls, R.J., 2015. Climate change adaptation frameworks: an evaluation
560 of plans for coastal Suffolk, UK. *Natural Hazards Earth System Science*, 15, 2511–2524.

561 Bates, P.D., Dawson, R.J., Hall, J.W., Horritt, M.S., Nicholls, R.J., Wicks, J., 2005. Simplified two-
562 dimensional numerical modelling of coastal flooding and example applications. *Coastal*
563 *Engineering*, 52 (9), 793–810.

564 Bell, P.S., Bird, C.O., Plater, A.J., 2016. A temporal waterline approach to mapping intertidal areas
565 using X-band marine radar. *Coastal Engineering*, 107, 84–101.

566 Bird, C.O. Bell, P.S. Plater, A.J., 2017a. Application of marine radar to monitoring seasonal and
567 event-based changes in intertidal morphology. *Geomorphology*, 285, 1–15.

568 Bird, C., Sinclair, A., Bell, P., 2017b. Radar-based nearshore hydrographic monitoring. *Hydro*
569 *International*, 21(2), 19–21, available online at [https://www.hydro-](https://www.hydro-international.com/content/article/radar-based-nearshore-hydrographic-monitoring)
570 [international.com/content/article/radar-based-nearshore-hydrographic-monitoring](https://www.hydro-international.com/content/article/radar-based-nearshore-hydrographic-monitoring)
571 [assessed 27th October 2017].

572 Brown, J.M., Knight, P., Prime, T., Phillips, B., Lyddon, C., Leonardi, N., Morrissey, K., Plater, A.J.,
573 2017. Science based tools informing coastal management in a changing climate.
574 *Proceedings Coastal Dynamics*, ASCE, Helsingør, Denmark, 12-16 June 2017, 12pp.

575 Brown, J.M., Phelps, J.J.C, Barkwith, A., Hurst, M.D., Ellis, M.A., Plater, A.J., 2016. The effectiveness
576 of beach mega-nourishment, assessed over three management epochs. *Journal of*
577 *Environmental Management*, 184 (2), 400–408.

578 Brown, J.M., Souza, A.J., Wolf, J., 2010. An 11-year validation of wave-surge modelling in the Irish
579 Sea, using a nested POLCOMS-WAM modelling system. *Ocean Modelling*, 33, 118–128.

580 Castelle, B., Marieu, V., Bujan, S., Splinter, K.D., Robinet, A., Sénéchal, N., Ferreira, S., 2015. Impact
581 of the winter 2013–2014 series of severe Western Europe storms on a double-barred sandy
582 coast: beach and dune erosion and megacusp embayments. *Geomorphology*, 238, 135–148.

583 ECMWF. 2016. European Centre for Medium Range Weather Forecasts. IFS Documentation,
584 European Centre for Medium Range Weather Forecasts: Reading, UK.

585 Energy Networks Association, 2009. ENA Annual Review. 26pp, available online at
586 <http://www.energynetworks.org/assets/files/news/publications/ENAREview2009.pdf>
587 [Accessed 24 January 2018].

588 Guangwei, H., 2011. Time lag between reduction of sediment supply and coastal erosion.

589 International Journal of Sediment Research, 26 (1), 27–35

590 Hawkes, P.J., Gouldby, B.P., 1998. The joint probability of waves and water levels: JOIN-SEA User
591 manual V1.0.

592 Jevrejeva, S., Moore, J.C., Grinsted, A., 2012. Sea level projections to AD2500 with a new
593 generation of climate change scenarios. *Glob. Planet. Change*, 80: 14–20.

594 Knight, P.J., Prime, T., Brown, J.M., Morrissey, K., Plater, A.J., 2015. Application of flood risk
595 modelling in a web-based geospatial decision support tool for coastal adaptation to climate
596 change. *Nat. Hazards Earth Syst. Sci.*, 15: 1457-1471.

597 Lam, J.S., Liu, C., Gou, X. 2017. Cyclone risk mapping for critical coastal infrastructure: Cases of
598 East Asian seaports. *Ocean & Coastal Management*, 141, 43–54.

599 Lewis, M., Bates, P., Horsburgh, K., Neal, J., Schumann, G., 2013. A storm surge inundation model
600 of the northern Bay of Bengal using publicly available data. *Quarterly Journal of the Royal
601 Meteorological Society*, 139 (671), 358–369.

602 Lotzel, H.K., Lenihan, H.S., Bourque, B.J., Bradbury, R.H., Cooke, R.G., Kay, M.C., Kidwell, S.M., Kirby,
603 M.X., Peterson, C.H., Jackson, J.B.C., 2006. Depletion, Degradation, and Recovery Potential
604 of Estuaries and Coastal Seas. *Science*, 312 (5781), 1806 –1809.

605 Lowe J, Howard T, Pardaens A, Tinker J, Holt J, et al. (2009) UK Climate Projections science report:
606 Marine and coastal projections, available online at <http://nora.nerc.ac.uk/9734/> [Accessed
607 20 June 2014].

608 Lyddon, C., Knight, P., Leonardi, N., Brown, J.M., Plater, A.J., 2017. Flood Hazard Sensitivity to
609 Storm Surge-High Water Concurrence in a Hyper-Tidal Estuary. *Proceedings of Coastal
610 Dynamics*, ASCE, Helsingør, Denmark, 12pp.

611 McCabe, M.V., Stansby, P.K., Apsley, D.D., 2013. Random wave runup and overtopping a steep sea
612 wall: Shallow-water and Boussinesq modelling with generalised breaking and wall impact
613 algorithms validated against laboratory and field measurements. *Coastal Engineering*, 74:
614 33–49.

615 McCall, R.T., Masselink, G., Poate, T.G., Roelvink, J.A., Almeida, L.P., 2015. Modelling the
616 morphodynamics of gravel beaches during storms with XBeach-G. *Coastal Engineering*, 103:
617 52–66.

618 McCall, R.T., Masselink, G., Poate, T.G., Roelvink, J.A., Almeida, L.P., Davidson, M., Russell, P.E.,
619 2014. Modelling storm hydrodynamics on gravel beaches with XBeach-G, *Coastal
620 Engineering*, 91: 231–250.

621 McMillan, A., Batstone, C., Worth, D., Tawn, J., 2011. Coastal flood boundary conditions for UK
622 mainland and islands. Project SC060064/TR2: Design sea levels.

623 Morrissey, K., Plater, A., Dean, M., 2018. The cost of electric power outages in the residential
624 sector: A willingness to pay approach. *Applied Energy*, 212, 141–50.

625 Narayan, S., Hanson, S., Nicholls, R. J., Clarke, D., Willems, P., Ntegeka, V., Monbaliu, J., 2012. A
626 holistic model for coastal flooding using system diagrams and the Source-Pathway-Receptor
627 (SPR) concept. *Natural Hazards and Earth System Science*, 12, 1431–1439.

628 Phillips, B., Brown, J., Bidlot, J.-R., Plater, A., 2017. Role of beach morphology in wave overtopping
629 hazard assessment. *Journal of Marine Science and Engineering*, 5 (1), 18 pp.

630 Plater, A.J., Brown, J.M., 2016. Building coastal resilience to sea-level rise and storms in the UK.
631 *Living With Environmental Change, Policy and Practice Note 30*, May 2016, 4pp,
632 www.nerc.ac.uk/research/partnerships/lwec/products/ppn/ppn30/ [assessed 20th Feb
633 2017].

634 Poate, T.G., McCall, R.T., Masselink, G. 2016. A new parameterisation for runup on gravel beaches.
635 *Coastal Engineering*, 117, 176–190.

636 Prime, T., Brown, J.M., Plater, A.J., 2015a. Physical and economic impacts of sea-level rise and low
637 probability flooding events on coastal communities. *PLOS ONE*, 10 (2),
638 e0117030.10.1371/journal.pone.0117030.

639 Prime, T., Brown, J.M., Plater, A.J., Dolphin, T., Fernand, L., 2015b. Morphological Control on
640 Overwashing Hazard at Multiple Energy Generation Installations. 14th International
641 workshop on wave hindcasting and forecasting and 5th Coastal hazards symposium, 8 - 13
642 November 2015, Key West, United States, 9pp, available online at
643 <http://www.waveworkshop.org/14thWaves/index.htm> [Accessed 24 January 2018].

644 Prime, T., Brown, J.M., Plater, A.J., 2016. Flood inundation uncertainty: The case of a 0.5% annual
645 probability flood event. *Environmental Science and Policy*, 59, 1–9.

646 Pringles, R., Olsina, F., Garcés, F., 2015. Real option valuation of power transmission investments
647 by stochastic simulation. *Energy Economics*, 47, 215–26.

648 Prime, T., Morrissey, K., Brown, J., Plater, A., 2018. Protecting Energy Infrastructure against the
649 Uncertainty of Future Climate Change: A Real Options Approach, *Journal of Ocean and
650 Coastal Economics*, in press June 2018.

651 Ratter, B.M.W., Petzold, J., Sinane, K., 2016. Considering the locals: coastal construction and
652 destruction in times of climate change on Anjouan, Comoros. *Natural Recourses Forum*, 40,

653 112–126.

654 Reichl, J., Schmidthaler, M., Schneider, F., 2013. The value of supply security: the costs of power
655 outages to Austrian households, firms and the public sector. *Energy Economics*, 36, 256–61.

656 Roelvink, D., Reniers, A., Van Dongeren, A., Van Thiel de Vries, J., Lescinski, J., McCall, R., 2010.
657 XBeach model description and manual. Unesco-IHE Inst. Water Educ. Deltares Delft Univ.
658 Technology.

659 Sayers, P.B., Hall, J.W., Meadowcroft, I.C., 2002. Towards risk-based flood hazard management in
660 the UK. *Proceedings of the Institution of Civil Engineers*, 150, 36–42.

661 Silva, S.F., Martinho, M., Capitão, R., Reis, T., Fortes, C.J., Ferreira, J.C., 2017. An index-based
662 method for coastal-flood risk assessment in low-lying areas (Costa de Caparica, Portugal).
663 *Ocean & Coastal Management*, 144, 90–104.

664 Wadey, M.P., Cope, S.N., Nicholls, R.J., McHugh, K., Grewcock, G., Mason, T., 2017. Coastal flood
665 analysis and visualisation for a small town. *Ocean & Coastal Management*, 116, 237–247.

666 Wadey, M., Haigh, I.D., Nicholls, R.J.; Brown, J.M., Horsburgh, K., Carroll, B., Gallop, S., Mason, T.,
667 Bradshaw, E., 2015. A comparison of the 31 January–1 February 1953 and 5–6 December
668 2013 coastal flood events around the UK. *Frontiers in Marine Science*, 2.
669 84.10.3389/fmars.2015.00084.